

See discussions, stats, and author profiles for this publication at: <https://www.researchgate.net/publication/329545710>

Comparative ultrastructure of the spermatogenesis of three species of Poecilosclerida (Porifera, Demospongiae)

Article in *Zoomorphology* · December 2018

DOI: 10.1007/s00435-018-0429-4

CITATION

1

READS

72

4 authors:



Vivian Vasconcellos

Universidade Federal da Bahia

6 PUBLICATIONS 118 CITATIONS

[SEE PROFILE](#)



Philippe Willenz

Royal Belgian Institute of Natural Sciences

85 PUBLICATIONS 1,200 CITATIONS

[SEE PROFILE](#)



Alexander V Ereskovsky

French National Centre for Scientific Research

202 PUBLICATIONS 3,317 CITATIONS

[SEE PROFILE](#)



Emilio Lanna

Universidade Federal da Bahia

31 PUBLICATIONS 228 CITATIONS

[SEE PROFILE](#)

Some of the authors of this publication are also working on these related projects:



Organization and patterning of sponge epithelia [View project](#)



Sponges from Peru - Esponjas del Perú [View project](#)



Comparative ultrastructure of the spermatogenesis of three species of Poecilosclerida (Porifera, Demospongiae)

Vivian Vasconcellos^{1,2} · Philippe Willenz^{3,4} · Alexander Ereskovsky^{5,6} · Emilio Lanna^{1,2}

Received: 15 August 2018 / Revised: 26 November 2018 / Accepted: 30 November 2018
© Springer-Verlag GmbH Germany, part of Springer Nature 2018

Abstract

The spermatogenesis of Porifera is still relatively poorly understood. In the past, it was accepted that all species presented a primitive-type spermatozoon, lacking special structures and acrosome. Nonetheless, a very peculiar spermatogenesis resulting in a sophisticated V-shaped spermatozoon with an acrosome was found in Poecilosclerida. This finding called into question the diversity and evolution of sperm cells in Poecilosclerida and in Porifera, as a whole. Is this sophisticated spermatozoon widespread in the group? We investigated here the ultrastructure of the spermatogenesis of three different species of Poecilosclerida (Demospongiae): *Iophon proximum*, *I. piceum*, and *Tedania ignis*. In all three species, spermatogenesis was synchronized within the spermatid cysts. *Iophon proximum* and *T. ignis* presented elongated sperm cells, but in *I. piceum*, their shape was oblong. A structure resembling an acrosome was only found in *T. ignis*. All three species presented modified spermatozoa, as in the majority of poecilosclerids investigated so far. Therefore, we are proposing that the elongated shape (modified type) of spermatozoon is the ancestral state based in the current phylogeny of Poecilosclerida and that the V-shaped sperm is only found in Crambeidae.

Keywords Reproduction · Sponges · Gametogenesis · Modified spermatozoa · Acrosome

Abbreviations

MNRJ Museu Nacional do Rio de Janeiro, Brazil
RBINS Royal Belgian Institute of Natural Sciences

✉ Emilio Lanna
emiliolanna@gmail.com

¹ Instituto de Biologia, Universidade Federal da Bahia, Rua Barão de Jeremoabo, s/n, Ondina, Salvador, BA 40170-115, Brazil

² National Institute of Science and Technology in Interdisciplinary and Transdisciplinary Studies in Ecology and Evolution (INCT IN-TREE), Salvador, Brazil

³ Royal Belgian Institute of Natural Sciences, Taxonomy and Phylogeny, 29 Rue Vautier, 1000 Brussels, Belgium

⁴ Laboratoire de Biologie Marine, Université Libre de Bruxelles, Avenue F.D. Roosevelt 50, 1000 Brussels, Belgium

⁵ Mediterranean Institute of Biodiversity and Ecology (IMBE), Aix Marseille Université, CNRS, IRD, Avignon Université, Station Marine d'Endoume, Rue de la Batterie des Lions, 13007 Marseille, France

⁶ Department Embryology, Faculty of Biology, Saint-Petersburg State University, Universitetskaya emb. 7/9, 199034 Saint-Petersburg, Russia

Introduction

Spermatogenesis is the process that gives rise to the male (usually motile) gamete of animals, i.e., the spermatozoon. In general, this process is characterized by the establishment of the germ line, successively followed by a proliferation of germ cells, production of spermatids by meiosis, and finally the differentiation of the mature spermatozoa (L'Hernault 2006; White-Cooper et al. 2009). Spermatozoa are among the most specialized of all metazoan cells. Their diverse and sometimes intricate morphologies are adapted to a primary function—the transmission of their own genetic contents to an egg of the same species (White-Cooper et al. 2009).

Sponges (Porifera) lack special organs or systems (Bergquist 1978; Simpson 1984) and their spermatogenesis occurs through the transdifferentiation of somatic cells into germ cells usually in non-specific regions of the animal body (Boury-Esnault and Jamieson 1999; Ereskovsky 2010). In Porifera, spermatocytes can either derive from archaeocytes or from choanocytes, but in most Demospongiae, spermatocytes are usually derived from choanocytes (Maldonado and Riesgo 2008; Riesgo and Maldonado 2009; Ereskovsky 2010). In this class, choanocytes will form aggregates progressively bordered by a follicular layer of pinacocyte-like

cells, forming the so-called spermatocysts (Reiswig 1983; Boury-Esnault and Jamieson 1999; Ereskovsky 2018). Spermatogenesis in sponges may either occur synchronously in all spermatocysts of a given specimen, or in a given population, or only within individual spermatocysts, independently from each other (Reiswig 1983). In general, as in other animals, sponges also present four spermatogenic stages: the first stage begins with spermatogonia, which undergo two consecutive divisions resulting in primary spermatocytes and secondary spermatocytes when the cells are kept interconnected by cytoplasmic bridges. During the third stage, these cells differentiate into haploid spermatids. Finally, at the fourth stage, spermatozoa become mature (Riesgo and Maldonado 2009; Ereskovsky 2010; Lanna and Klautau 2010).

Invertebrate spermatozoa can be divided into three types: (i) primitive; (ii) modified; and (iii) aberrant, the first two types being the most common ones (Hodgson 1986; Reunov 2005). The main differences among these types are the position/presence of different compartments of the cell, including acrosome, and the shape of the sperm. Although it has long been assumed that Porifera presented a primitive type of spermatozoa, currently a great diversity in their morphology and size is indubitable. Reiswig (1983) described at least 11 different shapes of sperm cells in Porifera. In most species of Poecilosclerida (Demospongiae) investigated so far, mature spermatozoa are elongated cells (Ereskovsky 2010). However, a different form of spermatozoa was found in this lineage: a sophisticated V-shaped form in *Crambe crambe* (Schmidt, 1862) (Riesgo and Maldonado 2009).

The order Poecilosclerida is one of the most speciose in the phylum Porifera, comprising four suborders, 25 families, 142 genera, and more than 2500 species (van Soest et al. 2018). However, neither the order, nor many of the inner clades are monophyletic (Redmond et al. 2013). As occurs in many other lineages of sponges, phylogenies based on molecular markers provide groups that have no morphological characteristics to support them, probably related to the homoplasy of the main characters used in the

taxonomy of Porifera (Redmond et al. 2013). This lack of congruence between molecules and morphology are not an exclusivity of sponges, but in other groups of metazoans, the use of the ultrastructure of the sperm cells in the phylogenies has helped to better understand the relationship among the clades (reviewed in Tudge 2009).

In addition, it has been postulated that the shape of the spermatozoon is influenced not only by the phylogenetic position of the species, but also by the physiological and functional demands during dispersal of the gamete and its subsequent fertilization process (Franzén 1956; Pitnick et al. 2009). In sponges, both the functional and phylogenetic significances of the diverse morphologies of the spermatozoa remain poorly understood. In addition to the variety of types of spermatozoa, there is no pattern for the origin of germ line in Poecilosclerida. In the carnivorous sponges *Esperiopsis koltuni* Ereskovsky and Willenz, 2007 and *Lycopodina occidentalis* (Lambe, 1893), as choanocytes are absent, the spermatocytes originate from archaeocytes (Riesgo et al. 2007a, b). A similar situation was suggested for the spermatogenesis of *Mycale fistulifera* (Row, 1911), even though this sponge has regular choanocyte chambers (Meroz and Ilan 1995). On the other hand, in *Myxilla incrustans* (Johnston, 1842), *Hemimycale columella* (Bowerbank, 1874), and *Crella elegans* (Schmidt, 1862), spermatocytes seem to originate from choanocytes (Efremova et al. 1987; Pérez-Porro et al. 2012). Expanding the number of species from different lineages of Poecilosclerida will help to understand the evolution of the group and also the usefulness of the ultrastructure of sperm cells to comprehend the phylogenetic relationship within this lineage of sponges. Therefore, in the present study, we compared the ultrastructure of the spermatogenesis of three species belonging to two different families of Poecilosclerida (Vargas et al. 2015): *Tedania ignis* (Duchassaing and Michelotti, 1864) (Fig. 1a), *Iophon proximum* (Ridley, 1881) (Fig. 1b), and *Iophon piceum* (Vosmaer, 1881) (Fig. 1c), found in the tropical, temperate, and polar zones of the world, respectively.

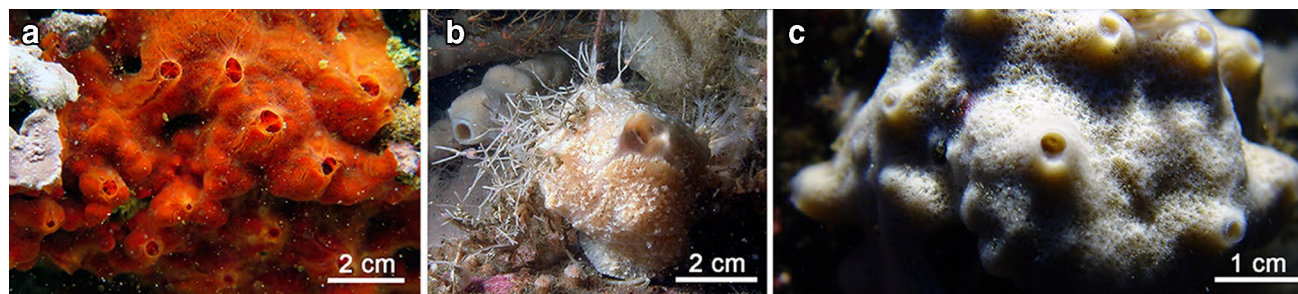


Fig. 1 In situ photographs of the investigated poecilosclerids: **a** *Tedania ignis* from Salvador, Brazil. **b** *Iophon proximum* from Comau Fjord, Chile. **c** *Iophon piceum* from White Sea, Russia

Materials and Methods

Seventeen tissue samples of *Tedania ignis* (with ca. 5 cm³) were collected at Porto da Barra, Salvador, Bahia, Brazil (13°00'15.2"S 38°32'00.2"W) in October 2014, January and November 2015, at 1–2 m depth. Despite its abundance, only one specimen of *Iophon proximum* (deposited as RBINS-IG 32,231-POR 8209 and MNRJ 8209) was collected in Comau Fjord, Southern Chilean Patagonia (42°24'9.66"S–72°25'14.01"W) in April 2004, at 25 m depth. Five specimens of *Iophon piceum* were collected near the White Sea Marine Biological Station «Belomorskaiskaya» of St. Petersburg State University (Kandalaksha Bay, White Sea) (66°17'N, 33°39'E), at 16 m depth in July 2002. While *T. ignis* was collected by snorkeling, both species of *Iophon* were sampled by SCUBA diving.

Specimens of *T. ignis* were processed for both light and electron microscopy. For light microscopy (LM), specimens were fixed in a solution of saline formaline (4%) for 24 h and processed for standard histology, as described in Lanna et al. (2018). For electron microscopy (EM), fragments were fixed (for at least 24 h at 4 °C) in a solution of 2.5% glutaraldehyde, 0.2 M of sodium cacodylate (pH 7.0) and filtered seawater (1:4:5) or fixed in a solution of 2.5% glutaraldehyde, 0.4 M PBS and 0.34 M NaCl (1:4:5). For scanning electron microscopy (SEM), fixed fragments were further rinsed with filtered seawater, dehydrated through a graded ethanol series, fractured in liquid nitrogen, thawed in 100% ethanol at ambient temperature and dried by the critical-point method from carbon dioxide before being mounted on aluminum stubs, coated with gold using a sputter coater, and observed with a JEOL (JSM-6390LV) scanning electron microscope at 12 kV. For transmission electron microscopy (TEM), fixed fragments were rinsed three times in 0.2 M sodium cacodylate buffer and post-fixed in a solution of 1% osmium tetroxide for 30 min at room temperature. Later, specimens were dehydrated in a graded acetone series and embedded in Epon. Semi-thin sections (1 µm thick) were stained with toluidine blue. Ultrathin sections (60–90 nm thick) double-stained with uranyl acetate and lead citrate (Reynolds 1963) were observed with a JEOL (JEM-1230) transmission electron microscope.

Specimens of both species of *Iophon* were also fixed for light and electron microscopy, but using different protocols. *Iophon piceum* specimens prepared for light microscopy were immersed in Bouin fixative. Vouchers were then dehydrated through an ethanol series, immersed in a celloidin–castor oil mixture and then in chloroform before embedding in paraffin. Thick sections (6 µm thick) were mounted on glass slides and stained with Mayer's hematoxylin, and eosin. For electron microscopy, fragments of about 1 mm³ were fixed in 2.5% glutaraldehyde in sodium

cacodylate buffer (pH 7.4) at room temperature for 1 h. After fixation, fragments were washed in phosphate buffer and post-fixed in 1% osmium tetroxide in phosphate buffer for 1 h. Samples were dehydrated through a graded ethanol series and embedded in Epon-Araldite.

Vouchers of *Iophon proximum* were fixed when arriving at the surface in 4% glutaraldehyde in 0.2 M sodium cacodylate buffer (pH 7.4) supplemented with 0.35 M sucrose and 0.1 M NaCl to obtain a final osmotic pressure of 1105 mOsM for 24 h at 4 °C. Vouchers were then washed six times for 10 min in 0.2 M sodium cacodylate buffer (pH 7.4) and post-fixed for 1 h in 1% osmium tetroxide in 0.2 M sodium cacodylate and 0.3 M NaCl, dehydrated through a graded ethanol series and embedded in ERL 4206 according to Spurr (1969).

For both *Iophon* species, sections were obtained with a diamond knife on a Leica Ultracut UCT ultramicrotome. Semi-thin sections (1 µm thick) were dried onto slides and stained with methylene blue borax. For TEM, thin sections were double-stained with uranyl acetate and lead citrate (Reynolds 1963) and later observed with a Tecnai 10 transmission electron microscope. For SEM, specimens were fractured in liquid nitrogen, critical-point-dried, sputter coated with gold–palladium and observed with a Philips (XL30 ESEM) scanning electron microscope.

Results

Tedania ignis

Tedania ignis is a simultaneous hermaphrodite and its spermatogenesis occurs all year round (Lanna et al. 2018). Spermatogenic cysts were rounded, enveloped by a single layer of follicle cells (Fig. 2a, b) and measured ca. 45 µm in diameter (Fig. 2b). They were spread in the choanosome without any clear pattern of distribution. Different stages of maturation occurred in the same individual, without synchronism between cysts, but the spermatogenic cells matured at the same time within each cyst. Somatic cells were seldom observed inside the spermatogenic cysts (Fig. 2c).

The first stages of spermatogenesis (spermatogonia and primary spermatocyte) were not observed in TEM. Nonetheless, we observed a progressive modification of the secondary spermatocyte. At first, the secondary spermatocytes were large cells (3.6 µm in diameter) with spherical shape, hyaline cytoplasm, and a large nucleus (2.1 µm in diameter). In this stage, the nucleus was rounded and its ratio to the cytoplasm was low. The chromatin was partially condensed and spread evenly in the nucleus (Fig. 2d). The cytoplasm presented a relatively well-developed Golgi apparatus and some spherical mitochondria (Fig. 2e).

Further on, the secondary spermatocyte comprised cells showing a volume reduction (2.2 µm in diameter) (Fig. 3a).

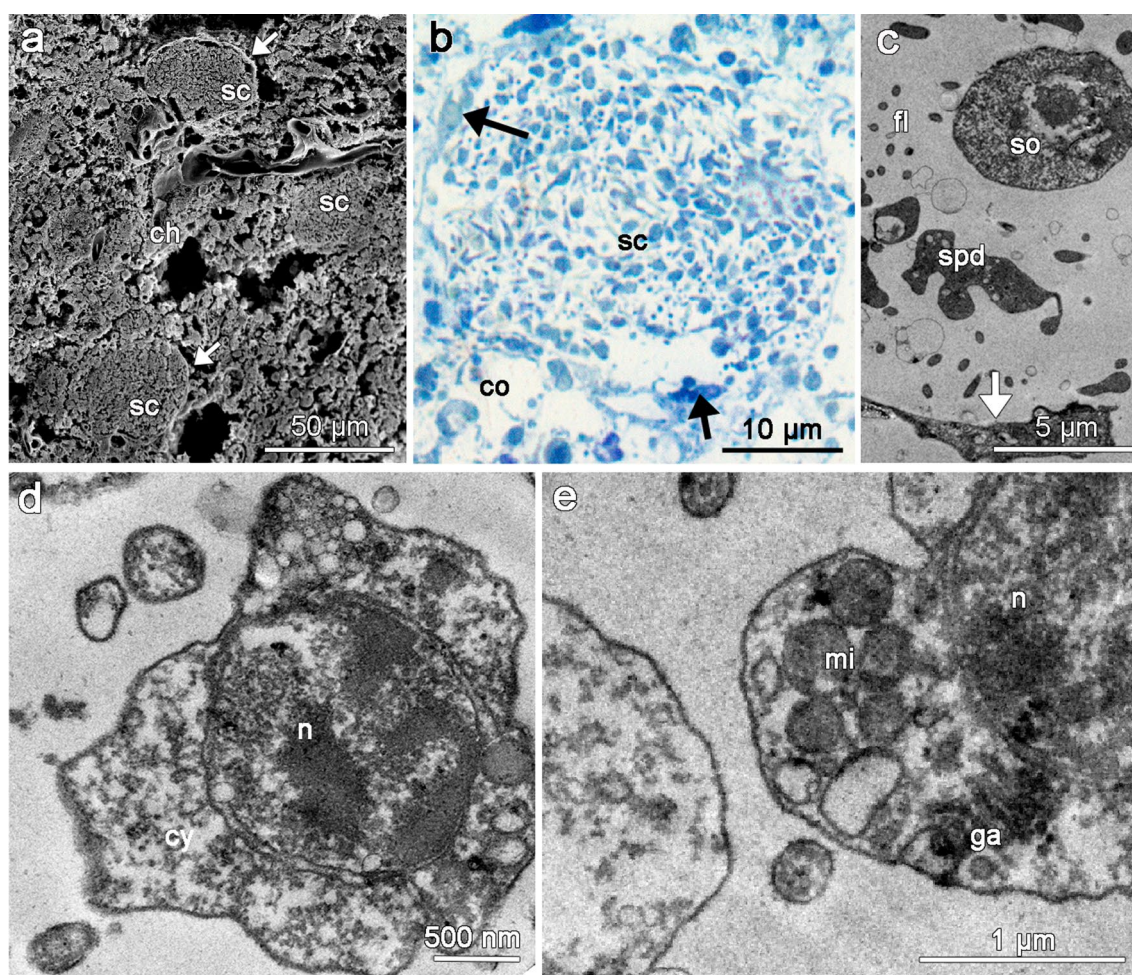


Fig. 2 *Tedania ignis*: Spermatic cysts and early secondary spermatocyte. **a** Choanosome (ch) with different spermatic cysts (sc) enveloped by a thin layer of follicle cells (cryofracture seen in SEM). **b** Spermatic cyst (sc) with spermatic cells developing in synchrony (LM). **c** Spermatids (spd), flagella (fl) and a large somatic cell (so)

within a late stage spermatic cyst (TEM). **d** Secondary-spermatocyte and its large nucleus (n) with compacting chromatin and clear cytoplasm (cy) (TEM). **e** Mitochondria (mi) and a Golgi apparatus (ga) in the cytoplasm of a secondary-spermatocyte. Arrows indicate follicle cells

At this stage, secondary spermatocytes were rounded, with a hyaline cytoplasm filled with small clear vesicles, a prominent Golgi apparatus and a rounded nucleus (Fig. 3b). Following the progression of development of the secondary spermatocyte, the cytoplasmic bridges kept the daughter cells connected. These cells became smaller ($< 2.0 \mu\text{m}$) than in the previous stages, the nucleus ratio to the cytoplasm was ca. 1:1, and the cytoplasm presented several small mitochondria. In this stage, the rounded nucleus started to condense, as some heterochromatin spots were observed in different areas (Fig. 3d). Following the second division, the secondary spermatocytes started to differentiate into spermatids, still connected through cytoplasmic bridges (Fig. 3c, f). However, dramatic changes occurred during this stage. The volume of the cytoplasm started to decrease, probably by shedding clear vesicles into the lumen of the spermatic cyst. Meanwhile, a flagellum started

to emerge close to the nucleus, which was still rounded (Fig. 3e). Later, while the condensation of chromatin progressed, the nucleus became elongated and an axoneme and some mitochondria were observed next to its basal region (Fig. 3f). In this early stage, the spermatid could present a curved shape (Fig. 3c, f, h), but when it further differentiated to become a sperm cell, the cytoplasm shedding induced the elongation of the cell, with mitochondria still rounded and gathered in the basal part of the cell body, next to the flagellum insertion (Fig. 3g). In the late spermatid stage, the nucleus was elongated, occupying most of the cytosol and an electron-dense material, likely pre-acrosomal vesicles, was present at the tip of the cell (between the plasma membrane and the apical portion of the nucleus), resembling a pre-acrosomal complex (Fig. 3i). No fully mature spermatozoon could be observed in electron microscopy despite the timing of the samples collections.

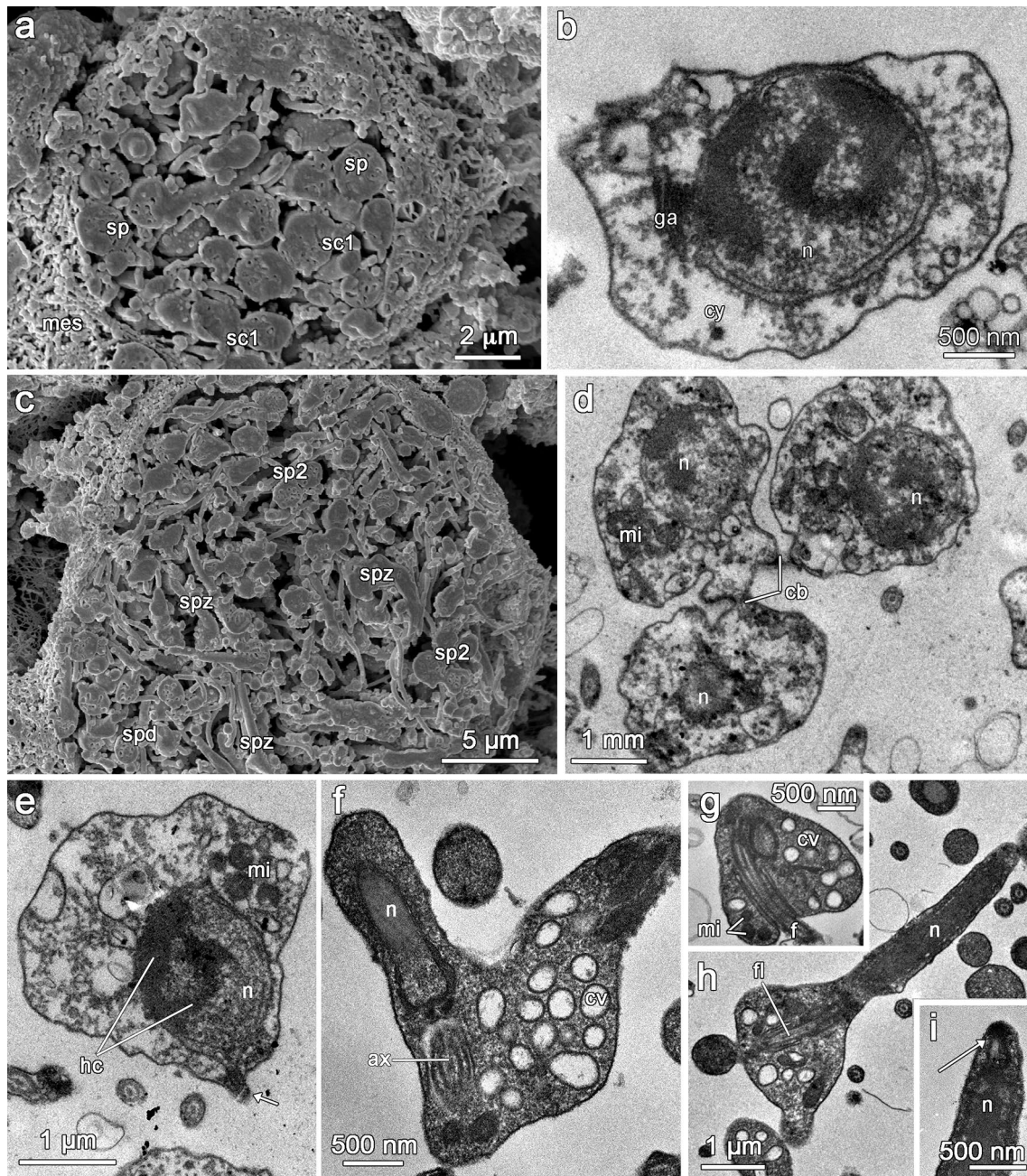


Fig. 3 *Tedania ignis*: Spermatocytes and spermatids. **a** Spermatogonia (sp) and primary spermatocytes (sc1) in a spermatogenic cyst (mes—mesohyl). **b** Secondary-spermatocyte with a large nucleus (n), clear cytoplasm (cy), and Golgi apparatus (ga). **c** Spermatogenic cyst with secondary spermatocytes (sp2), spermatids (spd), and spermatozoa (spz). **d** Secondary spermatocytes connected through cytoplasmic bridges (cb) (mi—mitochondria; n—nucleus). **e** Secondary spermatocyte in a late stage of transition towards spermatid, with compacting heterochromatin (hc) in the nucleus (n) (fl—flagellum; mi—mito-

chondria). **f** Mid-stage spermatid with cytoplasm containing many clear vesicles (cv). An elongated nucleus (n) is above the axoneme (ax). **g** Basal portion of the spermatid (neck) showing the flagellum (fl) emerging from the cytoplasm, several mitochondria (mi) and clear vesicles (cv). **h** Spermatid in a late stage, with stretched out nucleus (n) in the apical portion of the elongated cell. The base of the flagellum (fl) appears in the cytoplasm. **i** Tip of a late stage spermatid showing the pre-acrosomal vesicles (arrow) (n—nucleus)

Iophon proximum

In April 2004, the investigated specimens of *Iophon proximum* was actively carrying out its spermatogenesis. Spermatogenic cysts were rounded, measuring from 6 to 11 μm , and were covered by follicle cells and occurred in the choanosome of the sponges without any particular

localization (Fig. 4a). The follicle cells were flattened (Fig. 4b), with a lentil-like shape next to the nuclear region. The outward and inward surfaces of the follicle cells had numerous membrane protuberances (Fig. 4c). Maturation of the spermatogenic cells was not synchronous at the individual level but was evident within each spermatogenic cyst, encountered at different stages of spermatogenesis, from primary

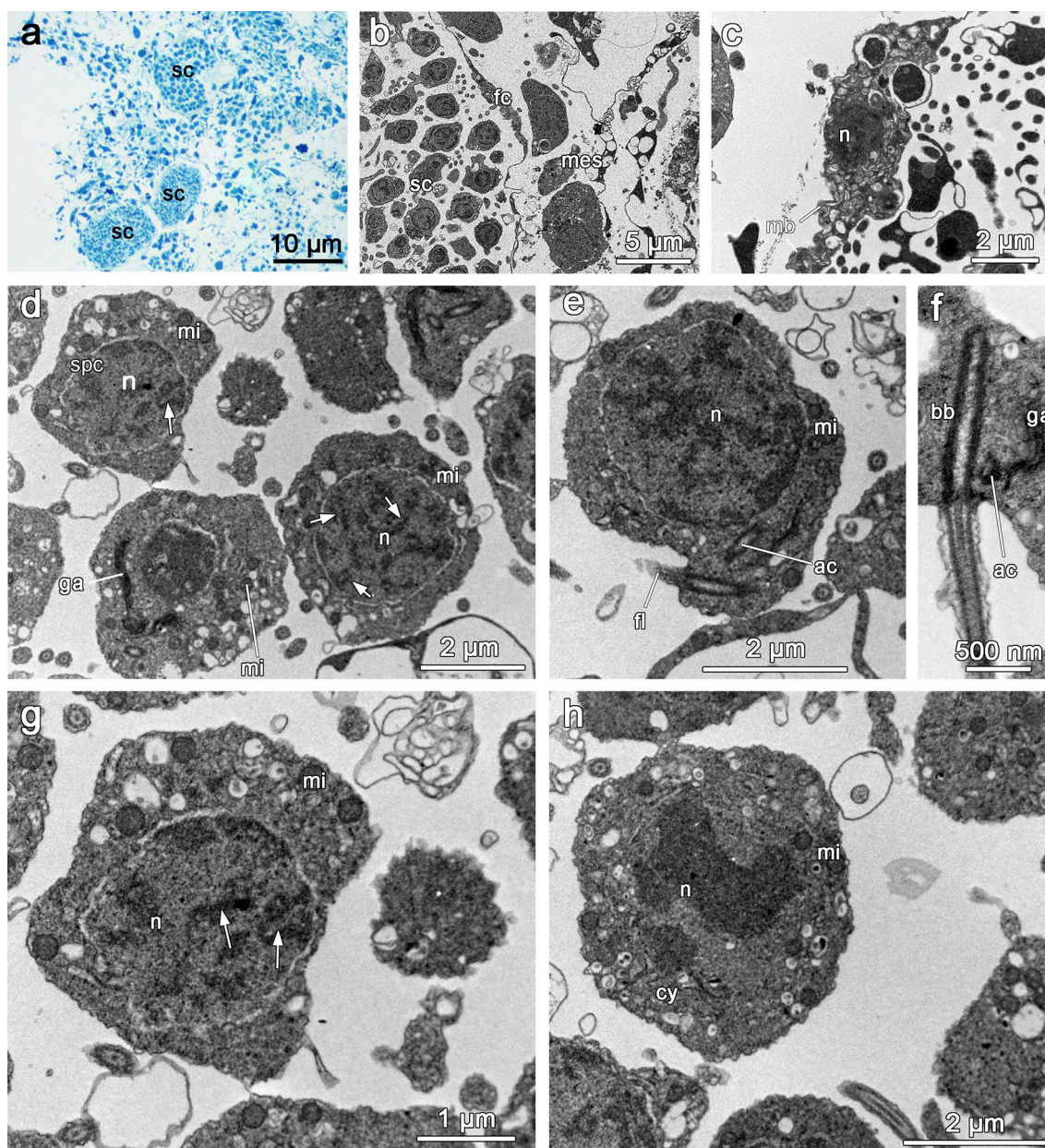


Fig. 4 *Iophon proximum*: Spermatogenic cysts, spermatogonia, and primary spermatocytes. **a** Spermatogenic cysts (sc) at different maturation stages in the choanosome. **b** Detail of a spermatogenic cyst (sc), (fc—follicle cells; mes—mesohyl). **c** Detail of a follicle cell with membranous protuberances (mb). **d** Spermatogonia with a large nucleus (n) with synaptonemal complexes (arrows) and Golgi apparatus (ga). **e** Primary spermatocyte showing basal body and accessory centriole

(ac) of the flagellum (fl). **f** Detail of the long basal body (bb) close to the Golgi apparatus (ga) and the accessory centriole (ac). **g** Primary spermatocyte with large nucleus (n) with compacting chromatin in patches (arrow—synaptonemal complex). **h** Secondary spermatocyte with a large nucleus (n) and compacting chromatin. Mitochondria (mi) are abundant in all stages

spermatocyte to mature spermatozoa. The early spermatogenic cysts development had already occurred when the sponges were collected and the spermatogonia origin could not be observed.

Primary spermatocytes presented numerous cytoplasmic inclusions and a flagellum. Mitochondria (0.25 μm in diameter) were round shaped with well-defined laminar cristae, the Golgi apparatus was large (1.7 μm long) with an irregular shape and consisted of 3–4 cisternae, synaptonemal complexes were present inside the nucleus, and several small electron-clear vesicles were visible in this stage (Fig. 4d, g). The flagella derived from large cytoplasmic outgrowths in one side of the cell. The flagellar basal apparatus was composed of a long basal body (1.05 μm long, 0.2 μm in diameter) to which an associated accessory centriole (0.71 μm long, 0.2 μm in diameter) and alar sheets were found. A rootlet was absent. The basal body was situated near the Golgi apparatus (Fig. 4e, f). The cell shape of the primary spermatocyte was not regular (3.8 μm in diameter), but a rounded nucleus (2.5 μm in diameter) was observed during this stage (Fig. 4g).

The first meiotic division was not synchronous, primary spermatocytes and secondary spermatocytes occurred at the same time within each cyst (Fig. 4g, h). The cytoplasm of the secondary spermatocytes was similar to the previous stage, but the cells were slightly smaller. The chromatin formed electron-dense areas in the nucleus (1.4 μm in diameter). Bi-nucleated cells could be observed after the second meiotic division, indicating the transition from secondary spermatocyte to spermatid stages (Fig. 5a), along with the formation of lipid droplets (Fig. 5b). The Golgi complex was not as long as in the previous stage, but consisted also of 3–4 cisternae (1.2 μm long). In this stage only, a cytoplasmic invagination forming a pit in the plasma membrane around the basal part of the flagellum was observed. Cytoplasmic bridges were still observed connecting secondary spermatocytes (Fig. 5c).

Later, secondary spermatocytes evolved into spermatids, acquiring an elongated shape (3.4 μm long, 1.3 μm in diameter) and being characterized by chromatin at different stages of condensation as well as a stretched nucleus in eccentric position (2.4 μm long, 0.9 μm in diameter). During this stage, pocket-like cytoplasmic invaginations arose around the basal portion of the flagella (Fig. 5d, e). The spermiogenesis was accompanied by the full compaction of the nuclear content altogether with the elongation of the nucleus. In addition, residual cytoplasm was shed at the basal side of the cell or alongside the flagellum reducing the overall volume of the cell (Figs. 5f, 6a). Spermatozoa were elongated (up to 4.2 μm long, with a diameter of 1.25 μm in basal and 0.83 μm in apical portion of the cell), with a long flagellum arising from a cytoplasmic invagination of variable depth (Fig. 6a, b). The anterior part of the nucleus presented a trapezoid shape in section. Mitochondria with constant spherical

shape and diameter (about 0.3 μm) occurred at the basal part of spermatozoa (Fig. 6b). No particular orientation of spermatozoa within spermatocysts was noticeable.

Iophon piceum

Iophon piceum is a simultaneous hermaphrodite, reproducing throughout the hydrological summer, i.e., late April to early October (Ereskovsky 2000). The spermatogenesis of this species was previously investigated in light and electron microscopy (Efremova et al. 1987) but the samples collected in 2002 are providing more information about the ultrastructure of its spermiogenesis, although only late stage of spermatogenic cysts were present (Fig. 7a). Spermatids and spermatozoa were enveloped by flattened cells of the spermatogenic cyst (Fig. 7a). Spermatids were rounded, measuring ca. 1.4 μm in diameter. The residual cytoplasm presented many large electron-clear vesicles and some tubules (likely resulting from the degenerating endoplasmic reticulum) specially found in the residual cytoplasmic bridges uniting two or more spermatids (Fig. 7b, c). At this stage, the nucleus was already fully condensed and started to stretch out, as well as the cell, which also gained an elongated shape. A decrease of the cell volume and large electron-clear vesicles started to appear in the cytoplasm (Fig. 7d). A single amorphous crystalline inclusion was then observed in different regions of the cell, but usually close to the nucleus (Fig. 7e–h). The flagellum of the spermatid/spermatozoon was long and free of ornamentation (Fig. 7a, b, e). Even though the insertion of the flagellum was not observed in an invagination of the cell membrane, small microvilli expansions were found at the basis of the flagellum in several sections (Fig. 7e, f, h, i). The accessory centriole was located close to the nucleus (Fig. 7d, f) and the basal body was positioned at the posterior end of the cell. Coarse microtubule fibers, supposedly related to the rootlet of the flagellum, spread from the basal body toward the nucleus. The nucleus reached ca. 3 μm in length and presented sharp endings in some sections, indicating a truncated tip of the cell (Fig. 7h).

Discussion

The morphology of several steps of the spermatogenesis of three species belonging to two different genera of Poecilosclerida inhabiting different regions of the globe (from tropics to polar regions) present sperm morphology with stark resemblance to each other and to other previously studied poecilosclerids. Their sampling was not spread over time and spermatogenesis was already in progress in all samples examined. Therefore, the cell lineage of the spermatogenic cells could not be determined. Nonetheless, based on the position, shape, and sizes of the spermatogenic cysts of the three

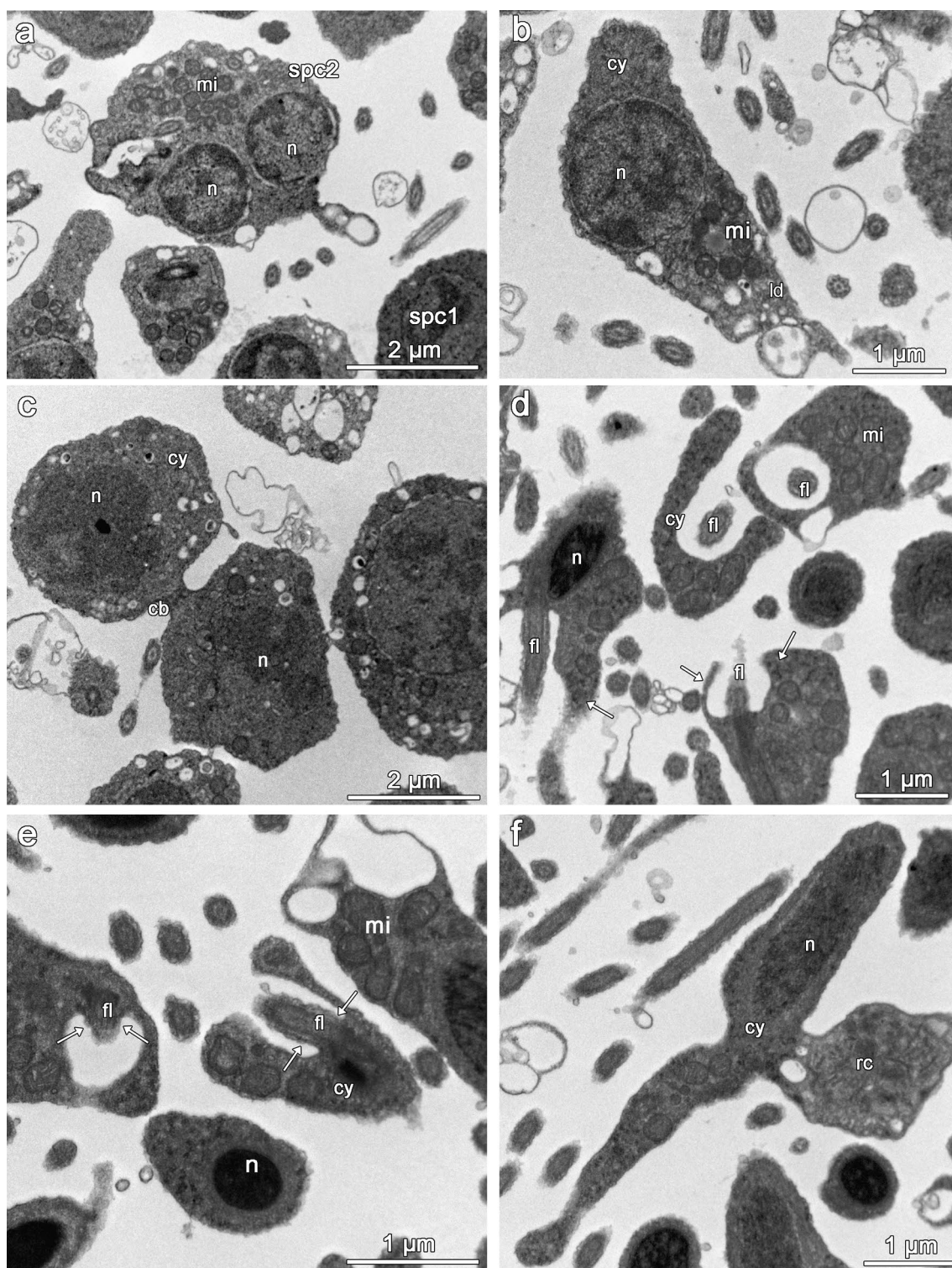


Fig. 5 *Iophon proximum*: Secondary spermatocytes and spermatids of *I. proximum*. **a** Secondary spermatocyte (spc2) soon after nuclear division. **b** Detail of a secondary spermatocyte with a large nucleus. **c** Two secondary spermatocytes united by cytoplasmic bridges (cb). **d** Spermatids with compacted and elongated nucleus and cytoplasm being shed. Several mitochondria (mi) are located in the putative neck

of the sperm cell and the flagellum (fl) is emerging from a deep pit (arrows) in the cytoplasm. **e** Detail of the neck of the spermatids with the flagellum insertion in the invagination of the cell (arrows). **f** Late spermatid with stretched nucleus and residual cytoplasm (rc) being shed alongside the cell (cy—cytoplasm; ld—lipid droplets; mi—mitochondria; n—nucleus; spc1—primary spermatocyte)

Fig. 6 *Iophon proximum*: Spermatozoon. **a** Spermatozoon (spz) with long flagellum seen in SEM. **b** TEM view of the spermatozoon showing compacted nucleus (n) with a trapezoid apical shape (fl—flagellum; mi—mitochondria)

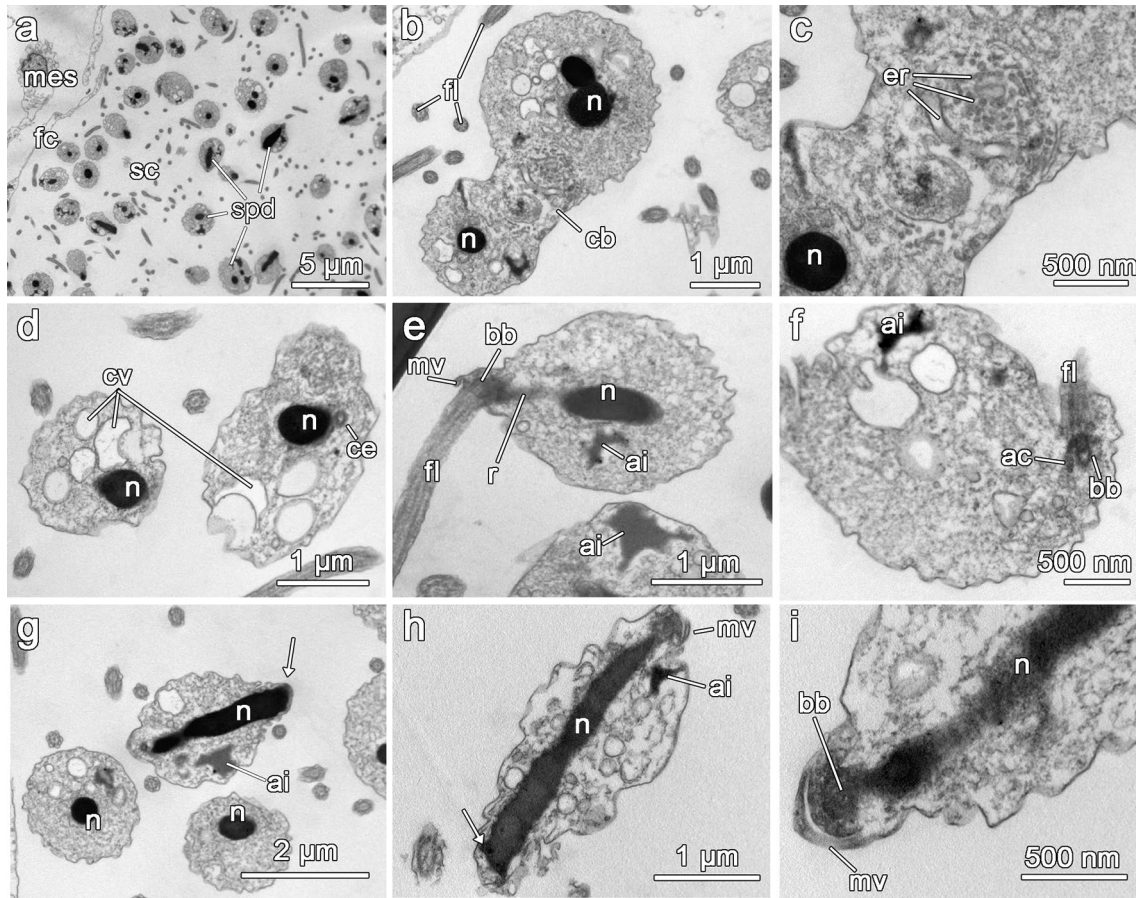
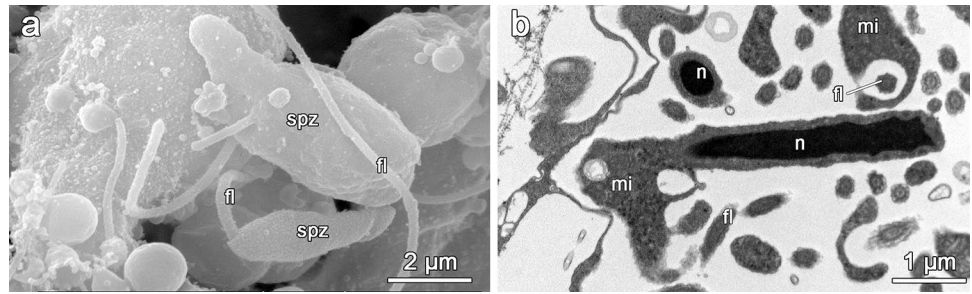


Fig. 7 *Iophon piceum*: Spermatids. **a** Overview of a spermatid cyst (sc) with spermatids (spd) (mes—mesohyl; fc—follicle cells). **b** Spermatids still connected by cytoplasmic bridges (cb). **c** detail of the cytoplasmic bridge seen in b, with the presence of several microtubules. **d** Spermatids containing important clear vesicles (cv). The centriole (ce) is inserted alongside the compacted nucleus. **e** Late spermatid with globular shape. A crystalline amorphous inclusion (ai) is located next to the compacted nucleus. The flagellum is

inserted in the neck of the cell attached to the basal body (bb). A fibrous rootlet (r) is connected to the nucleus. **f** Detail of the flagellum (fl) insertion showing the basal body (bb) and the accessory centriole (ac). **g** Amorphous inclusions are located in different regions of the cytoplasm. The tip of the nucleus bears a trapezoid shape (arrow). **h** Elongated spermatid with long nucleus and trapezoid apical shape (arrow). **i** Detail of the basal body (bb) and a microvilli (mv) at the neck of the spermatid (fl—flagellum; mv—microvilli; n—nucleus)

investigated species, we hypothesize that they also derive from choanocyte chambers, as showed previously for other poecilosclerids (Riesgo and Maldonado 2009; Pérez-Porro et al. 2012). As in *T. ignis* (and most Demospongiae), spermatogenesis in *Iophon proximum* and *I. piceum* took place

in spermatid cysts. The spermatogonia of *Tedania ignis* and also of *Iophon piceum* (Efremova et al. 1987) seemed to lose their flagella during the first division and to produce new ones at the later spermatid stage. This loss of flagellum was described in some other demosponges, like *Suberites massa*

Nardo, 1847 (Diaz and Connes 1980), *Spongia officinalis* Linnaeus, 1759 (Gaino et al. 1984), *Hippospongia lachne* (Laubenfels, 1936), *Spongia barbara* Duchassaing and Michelotti, 1864, *Spongia graminea* Hyatt, 1877 (Kaye and Reiswig 1991). However, in *Iophon proximum* the division of spermatocytes occurred without the loss of the flagellum. A similar situation is observed in another poecilosclerid, *C. crambe* (Riesgo and Maldonado 2009), and amongst some freshwater sponges (order Spongillida; class Demospongiae; Paulus 1989). In addition, the maintenance of flagella during spermatocyte division also occurs in sponges belonging to class Homoscleromorpha investigated so far (Gaino et al. 1986; Riesgo et al. 2007b; Ereskovsky 2010). This situation is in contradiction with most other Demospongiae and most Metazoa, where the flagellum appears only at the late stages of gametogenesis (Reunov and Hodgson 1994). Besides sponges, such situation was only observed in bivalves and the significance for the cell division is still not understood (Reunov and Hodgson 1994).

In the present study, the spermatozoa of all three species showed an elongate shape (about $5.8 \times 0.7 \mu\text{m}$ in *T. ignis*; $4.0 \times 0.9 \mu\text{m}$ in *I. piceum*; and $4.5 \times 0.8 \mu\text{m}$ in *I. proximum*). The morphology of their nucleus presented a striking similarity: in *T. ignis* as in the two *Iophon* species it was cylindrical with a wavy surface and a trapezium-like anterior end. Both *Iophon* species shared the presence of a shallow cytoplasmic invagination around the basal part of their sperm flagellum and an unusually elongated basal body (in *I. piceum* it was about $1.7 \mu\text{m}$ and in *I. proximum* $1.1 \mu\text{m}$). Within the order Poecilosclerida, former investigations in electron microscopy were carried out on *Myxilla incrustans* (Johnston, 1842), *Iophon piceum* (Efremova et al. 1987), *Lycopodina occidentalis* (Riesgo et al. 2007a, b), *Crambe crambe* (Riesgo and Maldonado 2009), *Hemimyscale columella* (Pérez-Porro et al. 2012), *Crellomima imparidens* (Rezvoi, 1925), and *Hymedesmia irregularis* Lundbeck, 1910 (Ereskovsky 2010). The ultrastructure of the spermatozoa of all three species investigated here was similar to that formerly observed for the sperm of *I. piceum* (Efremova et al. 1987) and of *L. occidentalis* (Riesgo et al. 2007a, b). In addition, the presence of a shallow invagination in the flagellum insertion of *I. proximum* and *I. piceum* is similar to that observed in the sperm cells of *H. columella* (Pérez-Porro et al. 2012). The presence of putative preacrosomal vesicles found in *T. ignis* was also observed in *Petrosia ficiformis* (Poiret, 1789) (Maldonado and Riesgo 2008). Nevertheless, the very sophisticated spermatozoon observed in *C. crambe* (V-shaped) (Riesgo and Maldonado 2009) was not observed in any of the three investigated species, and is still a peculiarity of this Mediterranean species. Apparently, *Crambe crambe* is found in a sister group of all other poecilosclerids investigated so far (Redmond et al. 2013; Vargas et al. 2015). Therefore, this sophisticated characteristic of the sperm of

C. crambe might be restricted to this species or, at least, to the lineage of the Crambeidae, rather than widely spread in Poecilosclerida as a whole. We expect that new investigations in other species of *Crambe* and of *Monanchora*, for example, are likely to answer this question.

Elongated and V-shaped spermatozoa with stretched out nucleus are considered as 'modified' and are widely regarded as a derived character in Metazoa (Reunov 2005). The co-occurrence of 'primitive' and 'modified' spermatozoa is a situation established in Porifera prior to the emergence of higher metazoans. The occurrence of 'modified' spermatozoa among Porifera sharing many ultrastructural traits with other metazoans could be explained by multiple cases of convergent evolution (Riesgo and Maldonado 2009). The same explanation, might also apply to the acrosome. Most spermatozoa of Porifera described until the end of the 1990s lacked an acrosome (Boury-Esnault and Jamieson 1999; Ereskovsky 2018) and it was commonly admitted that they all were of the 'primitive' type and were more basic than the primitive sperm of the majority of the other groups of metazoans. However, acrosomes were revealed in spermatozoa of Homoscleromorpha (Baccetti et al. 1986; Gaino et al. 1986), of two Calcarea species (Nakamura et al. 1998; Lanna and Klautau 2010) and also in several Demospongiae, especially Poecilosclerida (Riesgo et al. 2007a, b; Maldonado and Riesgo 2008; Riesgo and Maldonado 2009; Ereskovsky 2010). The spermatozoa of *T. ignis* presented small vesicles on top of the nucleus, that are likely pre-acrosomal vesicles, as in other Poecilosclerida (*L. occidentalis*, *C. crambe*, and *C. imparidens*) (Riesgo et al. 2007a, b; Riesgo and Maldonado 2009; Ereskovsky 2010). In contrast, in the spermatozoa of *I. piceum* and *I. proximum* these electron-dense granules were absent, as in *M. incrustans* (Efremova et al. 1987). Historically, the presence of acrosome in Porifera brought the following questions: is the acrosome a primitive organelle that disappeared during evolution in most orders, or is it a new organelle secondarily evolved in a few species? (Baccetti 1986). In the past, the sperm ultrastructure in sponges supported the hypothesis presented by Afzelius (1972) that primitive spermatozoa may have arisen twice, once in Porifera and a second time in all other metazoans. In this case, the sperm in Porifera seemed to have arisen primarily from choanocytes and has probably evolved independently of sperm in Cnidaria and other groups (Franzén 1996). However, it is now generally admitted that the spermatozoon is homologous in all Metazoa and that the absence of acrosome in most sponges could be a derived condition (Boury-Esnault and Jamieson 1999; Riesgo and Maldonado 2009). Apparently, the general shape of the sperm might be related more to the fecundation physiology of the animal, than being constrained by the phylogeny of the group. Although some similarities

could be observed amongst the three poecilosclerids investigated here, especially in the elongated shape of the sperm cell, the morphology of the spermatozoa of these species still present distinctive characteristics from each other. Expanding the investigations to other poecilosclerids is mandatory if we are to understand whether the diversity of sperm cell morphology is related to the phylogeny of the group or is an adaptation of the fertilization process. Nonetheless, until, these new studies investigating a large variety of species in different orders of the phylum is carried out, we suggest that the “modified” sperm (elongated with a basal flagellum) represents the ancestral state in Poecilosclerida. Further modifications in the morphology of the sperm, as the V-shaped ones of *C. crambe* (Riesgo and Maldonado 2009), are novelties within Poecilosclerida. We conclude that the current data about spermatozoa ultrastructure in Porifera as a whole (and in Poecilosclerida, particularly) is not sufficient to be used for taxonomy or phylogeny as already proposed in other groups of metazoans, e.g., annelids, insects, and birds (Tudge 2009). However, based on the shape of the spermatozoa, we can speculate that the fertilization (which is largely unknown in Demospongiae, Ereskovsky 2010) of these different species could be carried out in an apparently similar pattern.

Acknowledgements We would like to thank the staff at the Serviços de Microscopia Eletrônica-CPqGM-Fiocruz for help with the preparation of the samples of *T. ignis*. The present work is part of the PhD thesis of VV presented at the PPG em Diversidade Animal of the Federal University of Bahia. PhW and AE are indebted to Profs I. Eeckhaut and P. Flammang, Laboratoire de Biologie Marine, Université de Mons for their cordial reception in the TEM facilities under their care. Profs E. Pays and D. Pérez-Morga are also thanked for welcoming us in the Centre for Microscopy and Molecular Imaging of the Université Libre de Bruxelles. J. Cillis (RBINS) gave us technical support of with the SEM. We are grateful to G. Försterra and V. Häussermann (Huinay Scientific Field Station, Chile) and the Huinay Foundation without whom collecting *Iophon proximum* would not have been possible. Both are further thanked, as well as R. Fitzek and S. González for the hospitality and exceptional logistic support received at the Huinay Scientific Field Station. AE is grateful to the Marine Biological Station (ERS “Belomorskaia”) of St. Petersburg State University for technical support.

Funding EL and VV thank the Foundation for Researcher Support of the State of Bahia (FAPESB—Grant no. JCB0014/2016) and the National Council for Scientific and Technological Development (CNPq—Grant no. 477227/2013-9) for the financial assistance. This study was financed in part by the Coordenação de Aperfeiçoamento de Pessoal de Nível Superior—Brasil (CAPES)—Finance Code 001. The Belgian Federal Science Policy Office funded the work of AE at the RBINS (S&T Grant for collaboration with Oriental and Central Europe) as well as fieldwork of PhW in Chile (CALMARS I-contract EV/03/04B). This is publication Number 162 from the Huinay Scientific Field Station.

Compliance with ethical standards

Conflict of interest The authors declare that they have no conflict of interest. This article does not contain any studies with human participants performed by any of the authors. Brazilian sample collections were carried out under the license of ICMBIO (#9321-1). All applicable international, national, and/or institutional guidelines for the care and use of animals were followed.

References

- Afzelius BA (1972) Sperm morphology and fertilization biology In: Beatty RA, Gluecksohn-Waelsch S (eds) The genetics of the spermatozoon, pp 131–143
- Baccetti B (1986) Evolutionary trends in sperm structure. Comp Biochem Physiol 85A:29–36. [https://doi.org/10.1016/0300-9629\(86\)90457-3](https://doi.org/10.1016/0300-9629(86)90457-3)
- Baccetti B, Gaino E, Sarà M (1986) A sponge with acrosome: *Oscarella lobularis*. J Ultrastruct Mol Struct Res 94:195–198
- Bergquist P (1978) Sponges. Hutchinson, California
- Boury-Esnault N, Jamieson BGM (1999) Porifera. In: Adiyodi KG, Adiyodi RG (eds) Reproductive biology of invertebrates. Oxford & IBH Publishing, New Delhi, pp 1–41
- Diaz JP, Connes R (1980) Étude ultrastructurale de la spermatogenèse d’une démosponge. Biol Cell 38:225–230
- Efremova SM, Ereskovsky AV, Tokina DB (1987) Gametogenesis in sponges of the family Myxillidae from the White Sea. 2. Spermatogenesis in *Myxilla incrustans* and *Iophon piceus* (Demospongiae Poecilosclerida). Ontogenez 3:263–268
- Ereskovsky AV (2000) Reproduction cycles and strategies of the cold-water sponges *Halisarca dujardini* (Demospongiae, Halisarcida), *Myxilla incrustans* and *Iophon piceus* (Demospongiae, Poecilosclerida) from the White Sea. Biol Bull 198:77–87. <https://doi.org/10.2307/1542805>
- Ereskovsky AV (2010) The comparative embryology of sponges. Springer, Dordrecht. <https://doi.org/10.1007/978-90-481-8575-7>
- Ereskovsky AV (2018) Sponge reproduction. In: Skinner MK (ed), Encyclopedia of reproduction. vol. 6, Academic Press, Cambridge, pp. 485–490. <https://doi.org/10.1016/B978-0-12-809633-8.20596-7>
- Ereskovsky AV, Willenz Ph (2007) *Esperiopsis koltuni* sp. nov. (Demospongiae: Poecilosclerida: Esperiopsidae), a carnivorous sponge from deep water of the Sea of Okhotsk (North Pacific). J Mar Biol Assoc UK 87:1379–1386. <https://doi.org/10.1017/S0025315407058109>
- Franzén Å (1956) On spermiogenesis, morphology of spermatozoon and biology of fertilization among invertebrates. Zool Bidr Upp 3:355–482
- Franzén A (1996) Ultrastructure of spermatozoa and spermiogenesis in the hydrozoan *Cordylophora caspia* with comments on structure and evolution of the sperm in the Cnidaria and the Porifera. Invertebr Reprod Dev 29:19–26. <https://doi.org/10.1080/07924259.1996.9672491>
- Gaino E, Burlando B, Zunino L, Pansini M, Bulla P (1984) Origin of male gametes from choanocytes in *Spongia officinalis* (Porifera, Demospongiae). Int J Invert Rep Dev 7:83–93
- Gaino E, Burlando B, Buffa P, Sarà M (1986) Ultrastructural study of spermatogenesis in *Oscarella lobularis* (Porifera, Demospongiae). Int J Invert Rep Dev 10:297–305. <https://doi.org/10.1080/01688170.1986.10510253>

- Hodgson AN (1986) Invertebrate spermatozoa: structure and spermatogenesis. *Arch Androl* 17:105–114. <https://doi.org/10.3109/01485018608990179>
- Kaye HR, Reiswig HM (1991) Sexual reproduction in four Caribbean commercial sponges. I. Reproductive cycles and spermatogenesis. *Invertebr Repr Dev* 19:1–11
- L'Hernault SW (2006) Spermatogenesis. *WormBook* 1–14. <https://doi.org/10.1895/wormbook.1.85.1>
- Lanna E, Klautau M (2010) Oogenesis and spermatogenesis in *Paraleucilla magna* (Porifera, Calcarea). *Zoomorphology* 129:249–261. <https://doi.org/10.1007/s00435-010-0117-5>
- Lanna E, Cajado B, Santos da Silva C, da Hora J, Porto U, Vasconcellos V (2018) Is the Orton's rule still valid? Tropical sponge fecundity, rather than periodicity, is modulated by temperature and other proximal cues. *Hydrobiologia*. <https://doi.org/10.1007/s10750-018-3562-7>
- Maldonado M, Riesgo A (2008) Reproduction in the phylum Porifera: a synoptic overview. *Treballs de la SCB* 59:29–49. <https://doi.org/10.2436/20.1501.02.56>
- Maldonado M, Riesgo A (2009) Gametogenesis, embryogenesis, and larval features of the oviparous sponge *Petrosia ficiformis* (Haplosclerida, Demospongiae). *Mar Biol* 156:2181–2197. <https://doi.org/10.1007/s00227-009-1248-4>
- Meroz E, Ilan M (1995) Life history characteristics of a coral reef sponge. *Mar Biol* 124:443–451. <https://doi.org/10.1007/BF00363918>
- Nakamura Y, Okada K, Watanabe Y (1998) The ultrastructure of spermatozoa and its ultrastructural change in the choanocyte of *Sycon calcaravis* Hozawa. In: Watanabe Y, Fusetani N (eds) *Sponge sciences. Multidisciplinary perspectives*. Springer, Tokyo
- Paulus W (1989) Ultrastructural investigation of spermatogenesis in *Spongilla lacustris* and *Ephydatia fluviatilis* (Porifera, Spongillidae). *Zoomorphology* 109(3):123–130
- Pérez-Porro AR, González J, Uriz MJ (2012) Reproductive traits explain contrasting ecological features in sponges: the sympatric poecilosclerids *Hemimycale columella* and *Crella elegans* as examples. *Hydrobiologia* 687:315–330. <https://doi.org/10.1007/s10750-011-0919-6>
- Pitnick S, Hosken DJ, Birkhead TR (2009) Sperm morphological diversity. In: Birkhead TR, Hosken DJ, Pitnick S (eds) *Sperm biology: an evolutionary perspective*. Elsevier, Cambridge, pp 60–149
- Redmond NE, Morrow CC, Thacker RW (2013) Phylogeny and systematics of Demospongiae in light of new small-subunit ribosomal DNA (18S) sequences. *Integr Comp Biol* 53:388–415. <https://doi.org/10.1093/icb/ict078>
- Reiswig HM (1983) Porifera. In: Adiyodi KG, Adiyodi RG (eds) *Reproductive biology of invertebrates*. Oxford & IBH Publishing, New Delhi, pp 1–21
- Reunov AA (2005) Problem of terminology in characteristics of spermatozoa of Metazoa. *Russ J Dev Biol* 36:335–351. <https://doi.org/10.1007/s11174-005-0050-6>
- Reunov AA, Hodgson AN (1994) Ultrastructure of the spermatozoa of five species of south african bivalves (Mollusca), and an examination of early spermatogenesis. *J Morphol* 219:275–283. <https://doi.org/10.1002/jmor.1052190307>
- Reynolds ES (1963) The use of lead citrate at high pH as an electron-opaque stain in electron microscopy. *J Cell Biol* 17:208–212. <https://doi.org/10.1083/jcb.17.1.208>
- Riesgo A, Maldonado M (2009) An unexpectedly sophisticated, V-shaped spermatozoon in Demospongiae (Porifera): reproductive and evolutionary implications. *Biol J Linn Soc* 97:413–426. <https://doi.org/10.1111/j.1095-8312.2009.01214.x>
- Riesgo A, Taylor C, Leys SP (2007a) Reproduction in a carnivorous sponge: the significance of the absence of an aquiferous system to the sponge body plan. *Evol Dev* 9:618–631. <https://doi.org/10.1111/j.1525-142X.2007.00200.x>
- Riesgo A, Maldonado M, Durfort M (2007b) Dynamics of gametogenesis, embryogenesis, and larval release in a Mediterranean homosclerophorid demosponge. *Mar Freshwater Res* 58:398–417. <https://doi.org/10.1071/MF06052>
- Simpson TL (1984) *The cell biology of sponge*. Springer, New York, p 662. <https://doi.org/10.1007/978-1-4612-5214-6>
- Spurr AR (1969) A low-viscosity epoxy resin embedding medium for electron microscopy. *J Ultra Mol Struct R* 26:31–43. [https://doi.org/10.1016/S0022-5320\(69\)90033-1](https://doi.org/10.1016/S0022-5320(69)90033-1)
- Tudge C (2009) Spermatozoal morphology and its bearing on decapod phylogeny. In: Martin JW, Crandall KA, Felder DL (eds) *Decapod crustacean phylogenetics*. CRC Press, Boca Raton, pp 113–132
- van Soest RWM, Boury-Esnault N, Hooper JNA, Rützler K, de Voogd NJ, Alvarez B, Hajdu E, Pisera AB, Manconi R, Schönberg C, Klautau M, Picton B, Kelly M, Vacelet J, Dohrmann M, Díaz MC, Cárdenas P, Carballo JL, Ríos P, Downey R (2018) World Porifera database. <http://www.marinespecies.org/porifera>. Accessed 28 May 2018
- Vargas S, Kelly M, Schnabel K, Mills S, Bowden D, Wörheide G (2015) Diversity in a cold hot-spot: DNA-barcoding reveals patterns of evolution among Antarctic demosponges (Class Demospongiae, Phylum Porifera). *PLoS ONE* 10(6):e0127573. <https://doi.org/10.1371/journal.pone.0127573>
- White-Cooper H, Dogget K, Ellis RE (2009) The evolution of spermatogenesis. In: Birkhead TR, Hosken DJ, Pitnick S (eds) *Sperm biology: an evolutionary perspective*. Elsevier, Cambridge